Synthesis, Characterization, and Intervalence Charge Transfer Properties of a Series of Rhenium(I)−Iron(III) Mixed-Valence Compounds

Brian W. Pfennig,*,† Jamie L. Cohen,† Irene Sosnowski,‡ Nathan M. Novotny,‡ and Douglas M. Ho§,||

Department of Chemistry, Vassar College
124 Raymond Avenue, Poughkeepsie, New York 12604
and Department of Chemistry, Princeton University
Princeton, New Jersey 08544

Received October 2, 1998

Introduction

The properties of inorganic mixed-valence (MV) compounds, compounds which contain a reduced metal and an oxidized metal in electronic communication with each other, have been investigated in great detail since the Creutz−Taube ion was synthesized in the late 1960s.[1,2] A unique property of these species is the presence of a metal-to-metal charge-transfer (MM′CT) band in their electronic spectra which is absent from the spectra of the pure molecular fragments. Irradiation into this MM′CT band leads to an optical electron-transfer process, which can be detected in either the transient absorption spectra of the compounds or by the subsequent decomposition of the redox product.[3,4] For Robin and Day Class II MV compounds,[5] in which the transferring electron is localized on one or the other redox center, the energy of the MM′CT band, E_{op}, can be calculated by using classical Marcus−Hush theory[6] from the ground-state free energy difference, $\Delta G°$, and the reorganization energy, χ, for the nuclear coordinates to relax back to their equilibrium geometries (eq 1). Cyanide is frequently used as

$$E_{op} = \Delta G° + \chi \quad (1)$$

the bridging ligand, since MLCT bands associated with this strong field ligand typically occur at high energies[7] and do not interfere with the observation and identification of the lower-energy MM′CT transitions. Cyanide is also a good bridging ligand because of its ability to electronically mediate the optical electron-transfer process[8] and because the energy of ν(CN) depends on the metal to which it is attached, the nature of the linkage, the oxidation state of the metal, and whether it is a terminal or a bridging ligand.[9] Additionally, the redox potentials of cyanometalates have been shown to be dependent upon the coordinating nature of the solvent[10] and whether one or more of the cyanides is acting as a bridging ligand.[3,11] Coordination of the lone pair electrons on the cyanide nitrogen of a cyanometalate to an electron acceptor, such as H^+ or a transition metal, lowers the energy of the MCN π* molecular orbital and withdraws electron density from the C-bound metal, making it more difficult to oxidize that metal. This effect can be quite pronounced—often measuring in the hundreds of millivolts. We herein report the synthesis, characterization, and the exploitation of this unique property of cyanometalates in a series of cyanide-bridged $Fe^{III}-Re^{I}_n$ ($n = 1-3$) MV compounds. The energy of the $Re^{I}\rightarrow Fe^{III}$ MM′CT band in these complexes varies by 2850 cm^{-1} depending on the number of bridging cyanides, primarily as a result of this change in the standard reduction potential of the $Fe^{III/II}$ couple as a function of the number of covalently bound Re(I) metal centers.

Experimental Section

Materials and Instrumentation. $K_3Fe(CN)_6$, $Re(CO)_5Cl$, $AgOSO_2CF_3$, and 4,4′-dimethyl-2,2′-bipyridine (dmb) were purchased from Aldrich and used without further purification. 99.8% anhydrous acetonitrile (Aldrich) was measured by syringe just prior to its use in the electrochemical cell. Tetrabutylammonium hexafluorophosphate (Aldrich), used as the supporting electrolyte in the cyclic voltammetric experiments, was recrystallized twice from 95% ethanol before its use. All other solvents were reagent grade. Compounds $[dmbRe(CO)_3Cl]$ and $[dmbRe(CO)_3O_3SCF_3]$ were synthesized according to published procedures.[12,13]

Infrared absorption spectra (KBr pellets) were collected as the average of 16 scans by using a Perkin-Elmer 1600 Series FTIR with 2 cm^{-1} resolution. Electronic absorption spectra were collected in 1-cm quartz cuvettes at room temperature by using a Perkin-Elmer Lambda 900UV/vis/NIR or a Hewlett-Packard 8452A diode array spectrophotometer. Cyclic voltammograms were collected by using a standard three-electrode configuration and an EG&G PAR model 264A polarographic analyzer/stripping voltammeter. The potentiostat was coupled to a Power Macintosh computer running the LabVIEW program written by National Instruments. A gold button electrode was used as the working electrode, a Pt wire as the counter electrode, and a SSE electrode as the reference electrode. Cyclic voltammograms were recorded for each complex in 0.1 M $TBAH/CH_3CN$ electrolyte solutions at scan rates ranging from 20 to 500 mV/s. The accuracy of the reference electrode was checked using ferrocene as a standard.

Elemental analysis of cyanometalates by commercial laboratories is often difficult to obtain accurately due to the formation of metal carbides. To obtain reliable analyses, a suitable catalyst must be used.

* To whom correspondence should be addressed.
† Vassar College.
‡ Franklin and Marshall College.
§ Princeton University.
|| Responsible for single-crystal X-ray structure determination.

(1) Creutz, C.; Taube, H. *J. Am. Chem. Soc.* **1969**, *91*, 3938.
(2) (a) Creutz, C. *Prog. Inorg. Chem.* **1983**, *30*, 1. (b) Meyer, T. J. *Acc. Chem. Res.* **1978**, *11*, 94. (c) Taube, H. *Ann. N.Y. Acad. Sci.* **1978**, *313*, 483. (d) Meyer, T. J. *Ann. N.Y. Acad. Sci.* **1978**, *313*, 496.
(3) (a) Vogler, A.; Osman, A. H.; Kunkely, H. *Inorg. Chem.* **1987**, *26*, 2337. (b) Vogler, A.; Kunkely, H. *Ber. Bunsen-Ges. Phys. Chem.* **1975**, *79*, 301. (c) Vogler, A.; Osman, A. H.; Kunkely, H. *Coord. Chem. Rev.* **1985**, *64*, 159.
(4) Zhou, M.; Pfennig, B. W.; Steiger, J.; Van Engen, D.; Bocarsly, A. B. *Inorg. Chem.* **1990**, *29*, 2456.
(5) Robin, M. B.; Day, P. *Adv. Inorg. Chem. Radiochem.* **1967**, *10*, 247.
(6) (a) Marcus, R. A. *J. Chem. Phys.* **1956**, *24*, 966. (b) Marcus, R. A. *J. Chem. Phys.* **1965**, *43*, 679. (c) Marcus, R. A.; Sutin, N. *Inorg. Chem.* **1975**, *14*, 213. (d) Hush, N. S. *Trans. Faraday Soc.* **1956**, *57*, 557. (e) Hush, N. S. *Electrochim. Acta* **1968**, *13*, 1005. (f) Hush, N. S. *Chem. Phys.* **1975**, *10*, 361. (g) Hush, N. S. *Prog. Inorg. Chem.* **1967**, *8*, 357. (h) Hush, N. S. *Prog. Inorg. Chem.* **1967**, *8*, 391. (i) Bonvoisin, J.; Launay, J.-P.; Van der Auweraer, M.; De Schryver, F. C. *J. Phys. Chem.* **1994**, *98*, 5052.
(7) Lever, A. B. P. *Inorganic Electronic Spectroscopy*; Elsevier: Amsterdam, 1985.
(8) (a) Endicott, J. F.; Song, X.; Watzky, M. A.; Buranda, T.; Lei, Y. *Chem. Phys.* **1993**, *176*, 427. (b) Bignozzi, C. A.; Argazzi, R.: Schoonover, J. R.; Gordon, K. C.; Dyer, R. B.; Scandola, F. *Inorg. Chem.* **1992**, *31*, 5260.
(9) Nakamoto, K. *Infrared and Raman Spectra of Inorganic and Coordination Compounds*, 4th ed.; John Wiley and Sons: New York, 1986.
(10) Gutmann, V.; Gritzner, G.; Danksagmüller, K. *Inorg. Chim. Acta* **1976**, *17*, 81.
(11) Pfennig, B. W.; Bocarsly, A. B. *J. Phys. Chem.* **1992**, *96*, 226.
(12) Worl, L. A.; Duesing, R.; Chen, P.; Della Ciana, L.; Meyer, T. J. *J. Chem. Soc., Dalton Trans.* **1991**, 849.
(13) Sullivan, B. P.; Meyer, T. J. *J. Chem. Soc., Chem. Commun.* **1984**, 1244.

10.1021/ic9811751 CCC: $18.00
Published on Web 01/13/1999

The presence of additional transition metals adds a further complication. Therefore, the Re:Fe ratio in the samples below was measured directly by electron microprobe analysis (EPMA) using a CAMECA SX-50 instrument at the Princeton Materials Institute. This technique focuses a beam of electrons at a micron-sized area of the solid sample, exciting the inner-shell electrons of the material.[14] Upon relaxation back to the ground state, X-ray emission occurs which is characteristic of the elements present. Analyses were performed using an accelerating voltage of 15 kV and a regulated beam current of 20.3 nU. Fe_2O_3 and Re were used as the standards for the determination of Fe and Re, respectively. The results were reported as the Re/Fe ratio in the bulk of the sample. No attempt was made to analyze for N and C in this data set, and H is not detectable by EPMA.

Synthesis of $K_2[dmbRe(CO)_3(\mu\text{-}NC)Fe(CN)_5]$ (1). To 100 mL of an acetone solution containing 0.3723 g (0.76 mmol, 1.0 equiv) of $[dmbRe(CO)_3Cl]$ and 0.1957 g (0.76 mmol, 1.0 equiv) $AgOSO_2CF_3$ was added 25 mL of an aqueous solution containing 0.2500 g (0.76 mmol, 1.0 equiv) of $K_3Fe(CN)_6$. After the cloudy red-orange solution was stirred for 10 min at room temperature, it was heated to reflux for 45 min, during which time it changed to a dark reddish-brown color. The solution was then filtered hot through Celite to remove AgCl and concentrated by rotary evaporation to yield a green powder. This solution was filtered by vacuum and washed with two 10-mL portions of cold deionized water, followed by generous amounts of diethyl ether. The product was then dried at room temperature. The crude material was chromatographed on a silica gel column, using 1:2 acetone/methanol as the eluent and collecting the major band. The red-purple product was obtained by rotary-evaporation of the solvent. Re/Fe ratio (EPMA), 1.15 (theoretical, 1.00).

Synthesis of $K[dmbRe(CO)_3(\mu\text{-}NC)]_2[Fe(CN)_4]$ (2). To 100 mL of an acetone solution containing 0.7471 g (1.5 mmol, 2.0 equiv) of $[dmbRe(CO)_3Cl]$ and 0.3905 g (1.5 mmol, 2.0 equiv) $AgOSO_2CF_3$ was added 25 mL of an aqueous solution containing 0.2508 g (0.76 mmol, 1.0 equiv) $K_3Fe(CN)_6$. After the cloudy orange solution was stirred for 10 min at room temperature, it was heated to reflux for 45 min, during which time it changed to a dark brown color. The solution was then filtered hot through Celite to remove AgCl and concentrated by rotary evaporation to yield the crude product. This solution was filtered by vacuum and washed with two 10-mL portions of cold deionized water, followed by generous amounts of diethyl ether. The red-violet product was then purified by passing it through a silica gel column using 3:1 acetonitrile/water as the eluent, followed by rotary-evaporation of the solvent. Re/Fe ratio (EPMA), 2.00 (theoretical, 2.00).

Synthesis of $[dmbRe(CO)_3(\mu\text{-}NC)]_3[Fe(CN)_3]$ (3). To 100 mL of an acetone solution containing 1.1183 g (2.3 mmol, 3.0 equiv) of $[dmbRe(CO)_3Cl]$ and 0.5854 (2.3 mmol, 3.0 equiv) $AgOSO_2CF_3$ was added 25 mL of an aqueous solution containing 0.2503 g (0.76 mmol, 1.0 equiv) of $K_3Fe(CN)_6$. After the cloudy green solution was stirred for 10 min at room temperature, it was heated to reflux for 45 min, during which time it changed to a dark green-blue color. The solution was then filtered hot through Celite to remove AgCl and concentrated by rotary-evaporation to yield a green powder. This solution was filtered by vacuum and washed with two 10-mL portions of cold deionized water, followed by generous amounts of diethyl ether. The blue-violet product was obtained by elution from a silica gel column using a 1:1 acetone/methanol mixture, followed by rotary-evaporation of the solvent. Re/Fe ratio, 3.01 (theoretical, 3.00).

Synthesis of $[dmbRe(CO)_3(\mu\text{-}NC)]_3Fe(CN)_3\cdot 0.72CH_3COCH_3$ (4). A 2 mL amount of a 3.0 mM solution of $[dmbRe(CO)_3O_3SCF_3]$ in acetone was combined with 2.0 mL of a 1.0 mM aqueous solution of $K_3Fe(CN)_6$ in a small test tube, and the mixture was allowed to sit undisturbed in the dark at room temperature for 3 days. During this time, the solution gradually changed from a yellow into a red-violet color and precipitated short, thin brown-violet needles of the product. The crystals were kept in this solution in the dark until they were used for single-crystal X-ray diffraction. Then, they were gently collected in a Gooch crucible by vacuum filtration and washed with small amounts of ice-cold acetone.

Table 1. Relevant IR Absorptions (cm^{-1}) for Compounds **1**−**4** (KBr pellets) and Their Assignments

assignment	**1**	**2**	**3**	**4**
$\nu(CN)_{br}$	2146 w	2146 m	2145 m	2147 m
$\nu(CN)_{non}$	2116 m	2118 m	2118 vw	2121 sh
$\nu(CO)_{cis}$	2024 vs	2024 vs	2024 vs	2023 vs
$\nu(CO)_{trans}$	1903 br	1905 br	1912 br	1910 br
$\nu(Fe-CN)_{br}$	571 m	572 m	572 m	570 w
$\nu(Fe-CN)_{non}$	518 m	517 m	513 m	514 w

Crystal Structure Determination. A brown-violet needle of $[dmbRe(CO)_3(\mu\text{-}NC)]_3Fe(CN)_3\cdot 0.72CH_3COCH_3$, 0.02 × 0.08 × 0.20 mm in size, was mounted on a glass fiber with epoxy cement and then transferred to a Siemens P4 diffractometer equipped with an LT-2 low-temperature device and graphite-monochromated Mo Kα radiation (λ = 0.710 73 Å). Lattice parameters at 230 K were determined from the setting angles of 50 centered reflections having $3.89 \le \theta \le 9.86°$. Preliminary peak scans through reciprocal space revealed no systematic absences, indicating that the compound had crystallized in the triclinic space group $P1$ or $P\bar{1}$. The latter space group was selected on the basis of the observed mean $\bar{E}^2 - \bar{1}$ value of 0.917 (versus the expected value of 0.968 for centrosymmetric and 0.736 for noncentrosymmetric). One hemisphere of data ($+h, \pm k, \pm l$) was collected in the ω scan mode with θ ranging from 1.5 to 22.50° and with scan speeds varying from 4 to 8.00°/min. Three standards (011, 110, $10\bar{3}$) were measured for every 97 reflections and revealed a 7.56% drop in their mean intensity values over the course of the experiment. Corrections were made for the decay, as well as for Lorentz and polarization effects, but not for extinction. A semiempirical absorption correction based on ψ scans was also applied, with the minimum and maximum transmission factors being 0.7385 and 0.9342, respectively.

The structure was solved in the triclinic space group $P\bar{1}$ (No. 2) by heavy atom methods in the SHELXTL package of programs[15] and refined by full-matrix least-squares on F^2 using SHELXL-93.[16] Except where noted below, all of the non-H atoms were refined with anisotropic displacement coefficients, H atoms were included with a riding model and isotropic displacement coefficients $U(H) = 1.2U(C)$, and the weighting scheme employed was $w = 1/[\sigma^2(F_0^2) + (0.1202P)^2]$, where $P = (F_0^2 + 2F_c^2)/3$. The methyl H atoms were assigned $U(H) = 1.5U(C)$, and the methyl's refined as rotating groups. An acetone molecule was located and included with isotropic displacement coefficients and a common occupancy variable which refined to a value of 0.72(4). The scattering factors were taken from the *International Tables for Crystallography*, Vol. C.[17]

Results and Discussion

Characterization. The relevant IR absorptions of compounds **1**−**3** are listed in Table 1. The IR and UV/vis spectra of **3** and **4** are nearly identical, indicating that the two differ only in their degree of solvation. Each compound contains two ν(CN) stretches: one centered at ∼2120 cm^{-1} with a second peak at ∼2150 cm^{-1}. These peaks can be assigned to the nonbridging and bridging cyanide stretching frequencies, respectively, of cyanides which are C-bound to an Fe(III) atom, by analogy with similar compounds in the literature.[4,11,18] Bridging cyanide stretches typically occur at higher energies than nonbridging

(14) Goldstein, J. I., et. al. *Scanning Electron Microscopy and X-ray Microanalysis: A Text for Biologists, Materials Scientists, and Geologists*, 2nd ed.; Plenum Press: New York, 1992.

(15) Sheldrick, G. M. *SHELXTL-PLUS*, Release 4.21; Siemens Analytical X-ray Instruments, Inc.: Madison, WI, 1990.

(16) Sheldrick, G. M. *SHELXL-93*; *Program for the Refinement of Crystal Structures*; University of Göttingen: Germany, 1993.

(17) (a) Maslen, E. N.; Fox, A. G.; O'Keefe, M. A. *International Tables for Crystallography: Mathematical, Physical and Chemical Tables*; Kluwer: Dordrecht, The Netherlands, 1992; Vol. C., pp 476−516. (b) Creagh, D. C.; McAuley, W. J. *International Tables for Crystallography: Mathematical, Physical and Chemical Tables*; Kluwer: Dordrecht, The Netherlands, 1992; Vol. C, pp 206−222.

(18) Wu, Y.; Cochran, C.; Bocarsly, A. B. *Inorg. Chim. Acta* **1994**, *226*, 251.

Table 2. Peak Potentials (V vs SSE) and Their Assignments for Compounds **1**−**3** and dmbRe(CO)$_3$Cl in 0.1 M TBAH/CH_3CN Using a Au/Pt/SSE Electrode Configuration at a Scan Rate of 100 mV/s

compound	Re[a]	dmb[b]	Fe[c]
1	1.47	−1.49	0.15
2	1.49	−1.49	0.44
3	1.47	−1.49	0.71
dmbRe(CO)$_3$Cl	1.47	−1.44	NA

[a] The $Re^{I/II}$ couple was determined to be irreversible. The potentials listed are therefore anodic peak potentials. [b] The $dmb^{0/-}$ couple displayed larger cathodic waves than anodic ones, with typical peak-to-peak separations at 100 mV/s scan rate of 300 mV. The potentials cited were calculated as the midpoint between the oxidative and reductive waves. [c] The $Fe^{III/II}$ couple was determined to be quasi-reversible over the scan rates studied. The potentials cited were calculated as the midpoint between the oxidative and reductive waves.

CN stretches in complexes in which back-bonding is not a larger factor than the kinematic coupling imposed by restraining the CN vibration between two heavy metal atoms.[8b] The position of these CN stretches distinguishes them from Fe(II)-bound cyanides, which would appear at lower energies by ∼80 cm^{-1}, indicating that the oxidation state of the iron center in each of these complexes did not change during the course of the reaction. Two peaks at ∼570 and ∼515 cm^{-1} in the low-energy region of the IR spectrum for each of these complexes can be assigned as $Fe^{III}-CN_{br}$ and $Fe^{III}-CN_{non}$ by comparison with the literature. Furthermore, the ratio of the intensity of the bridging to the nonbridging CN stretch increases from compounds **1**−**3**, ranging from 0.51 for **1** to 0.79 for **2** to 2.5 for **3**. This qualitative relationship between the relative intensities of the two cyanide stretches and the number of attached Re(I) moieties supports a structural model in which the Re atoms are attached to the ferricyanide center by a coordinate covalent bond to the N end of a bridging cyanide ligand.

Each compound also possesses two very strong peaks in the carbonyl stretching region of the IR at ∼2025 and ∼1900 cm^{-1}. The peak at 2024 cm^{-1} is identical between compounds **1**−**3** and has previously been assigned as ν(CO) for the carbonyl ligands which are cis to the cyanide ligand.[19] The lower-energy peak is therefore assigned as ν(CO) for the CO which is trans to the bridging cyanide. The energy of this latter band gradually shifts to higher frequencies as the number of Re molecules attached to the central ferricyanide increases. The blue-shift implies that there is an decreased amount of back-bonding to the π^* CO ligand from the d^6 Re(I) center. Additionally, the relative intensities of the ratio of the ∼2025 ν(CO) peak to the combined ν(CN) stretches increases from 1.9 for **1** to 3.0 for **2** to 3.4 for **3**. These data reflect the increased number of CO stretches relative to CN stretches as the central ferricyanide becomes increasingly substituted with pendant dmbRe(CO)$_3^-$ groups.

Table 2 lists the peak potentials (V vs SSE) determined by cyclic voltammetry for compounds **1**−**3** at a scan rate of 100 mV/s. The anodic peak at ∼1.5 V for each complex has been assigned to the irreversible oxidation of Re(I) to Re(II). This peak occurs at 1.47 V for our sample of dmbRe(CO)$_3$Cl. Each of the three complexes also exhibits a quasi-reversible peak at ∼−1.5 V, which corresponds to the dmb/dmb$^{\bullet-}$ redox couple, determined as −1.44 V for dmbRe(CO)$_3$Cl. A third peak, assigned to the $Fe^{III/II}$ couple, varies significantly depending upon the number of pendant Re(I) groups, with half-wave potentials ranging from 0.15 V for **1** to 0.44 V for **2** to 0.71 V for **3**. This nearly monotonic positive shift in redox potentials as each subsequent cyanide bridges to a Re(I) molecule is analogous to that observed for a series of $Fe^{II}-CN-Pt^{IV}$ oligomers on a chemically modified electrode.[20] The redox potential of the Fe moiety in these $Fe^{II}-Pt^{IV}$ cyanide-bridged oligomers was dependent on the number of Pt(IV) units to which the Fe(II) was bridged, becoming more positive with each additional substitution. The peak-to-peak separations for the Fe redox waves of **1**−**3** was scan rate-dependent and increased with the Re/Fe ratio for any given scan rate. The anodic peak currents for the Fe and Re waves for **1** are roughly the same, whereas the Re wave increases in area relative to the Fe wave as the Re/Fe ratio increases from **1**−**3**, in qualitative agreement with the observed stoichiometry of these complexes. The presence of a single Fe wave for each of the three species, along with the EPMA data, supports the stoichiometric purity of these compounds. Although the Re/Fe ratio for **1** was somewhat greater than the theoretical value of 1.00, the electrochemistry of this complex exhibits a single Fe redox wave and the UV/vis data from several different samples of **1** are reproducible.

Table 3. Absorption Maximum (nm) of the MM′CT Absorption Band for Compounds **1**−**3** and Pertinent Solvent Parameters

solvent	$(1/D_{op} - 1/D_s)$	AN	**1**	**2**	**3**
acetone	0.493	12.5	484	506	534
acetonitrile	0.530	19.3	497	543	579
dimethylformamide	0.463	16.0	477	512	554
dimethyl sulfoxide	0.436	19.3	482	550	593
ethylene glycol	0.462	42.1	568	606	657
methanol	0.535	41.3	578	610	649
1-propanol	0.471	33.5	553	592	608
water	0.546	54.8	613	667	753

Table 4. Summary of Crystallographic Data for Compound **4**

empirical formula	$C_{51}H_{36}FeN_{12}O_9Re_3 \cdot 0.72C_3H_6O$
unit cell dimensions	$a = 13.140\ (1)$ Å
	$b = 14.905\ (2)$ Å
	$c = 18.941\ (2)$ Å
	$\alpha = 106.962\ (9)°$
	$\beta = 91.951\ (8)°$
	$\gamma = 106.424\ (8)°$
V	3375.9 (7) Å^3
Z	2
fw	1617.18
space group	$P\bar{1}$ (No. 2)
temperature	230(2) K
radiation	Mo Kα ($\lambda = 0.710\ 73$ Å)
density (calculated)	1.591 g/cm^3
absorption coefficient	56.27 cm^{-1}
max and min transmission coefficient	0.9342 and 0.7385
R, wR2 [$I > 2\sigma(I)$]	8.23%, 18.86%
R, wR2 (all data)	17.31%, 24.89%

Each of the MV compounds contains a single broad peak in the visible region (Table 3) at lower energy than any of the absorptions from dmbRe(CO)$_3$Cl or $K_3Fe(CN)_6$ alone, and is thus assigned as a MM′CT from $Re^I \rightarrow Fe^{III}$. Supporting the assignment of the lowest-energy visible absorption band for each complex as MM′CT is the fact that the substitution reaction of dmbRe(CO)$_3O_3SCF_3$ with $K_4Fe(CN)_6 \cdot 3H_2O$ to yield a cyanide-bridged Re^I-Fe^{II} complex, in which both metals are in reduced oxidation states, did not yield a new MM′CT peak in the absorption spectrum at energies lower than 450 nm. Furthermore, reduction of the colored mixed-valence compounds **1**−**3** with hydrazine hydrate gave yellow solutions, in which the

(19) Balk, R. W.; Stufkens, D. J.; Oskam, A. *J. Chem. Soc., Dalton Trans.* **1981**, 1124.

(20) Wu, Y.; Pfennig, B. W.; Bocarsly, A. B.; Vicenzi, E. P. *Inorg. Chem.* **1995**, *34*, 4262.

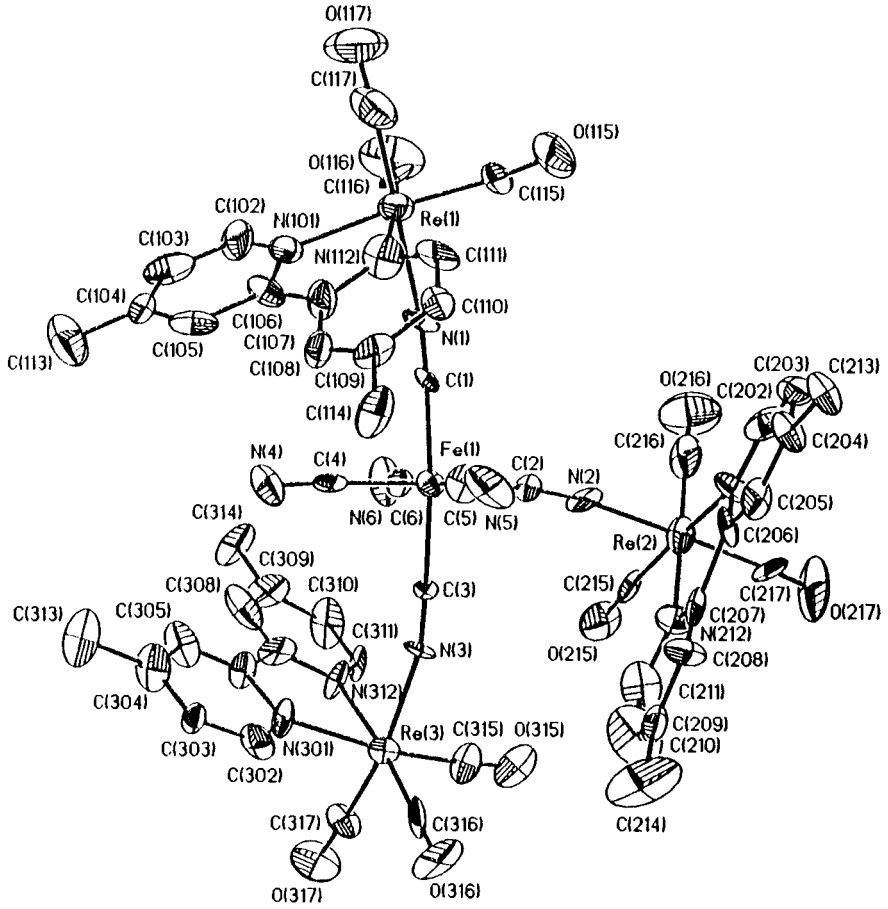

Figure 1. ORTEP drawing for the single-crystal X-ray study of Compound **4** using a Siemens P4 diffractometer.

MM′CT was no longer evident in the UV/vis spectra of these molecules. Given the positive shift in $\Delta G°$ in this series of compounds as n increases, the energy of the MM′CT band is expected to shift to lower energies. Compound **1** absorbs at 497 nm in acetonitrile solution, while **2** absorbs at 543 nm, and **3** absorbs at 579 nm, supporting the assignment of this lowest energy band as $Re^{I} \rightarrow Fe^{III}$ MM′CT. The molar absorptivities for these MM′CT peaks (smallest for **1** and largest for **3**) also corroborate the increased number of pendant Re molecules. The energies of the MM′CT bands in these complexes strongly depend on the solvent, as indicated by the data in Table 3. This is discussed in more detail in a later section of the paper.

Crystal Structure. A summary of the crystallographic data for **4** appears in Table 4. The ORTEP plot of the complex (excluding the acetone molecule which crystallizes as part of the unit cell) is shown in Figure 1, and the unit cell is depicted in Figure S1 in the Supporting Information. Atomic coordinates ($\times 10^4$) and equivalent isotropic displacement parameters ($Å^2 \times 10^3$) are listed in Table 5. The refinements converged to R(F) = 8.23%, wR(F^2) = 18.86%, and S = 1.07 for 4414 reflections with $I > 2\sigma(I)$; and R(F) = 17.31%, wR(F^2) = 24.89%, and S = 0.96 for 8681 unique reflections, 709 variables, and 84 restraints.[21] The molecular unit consists of a ferricyanide center, to which are attached three dmbRe(CO)$_3$- units in meridional geometry. Each Re moiety is facial with respect to its three carbonyl ligands, indicating that no other geometric rearrangement occurred during the substitution reactions. Selected bond angles for **4** are listed in Table 6. The average Fe−C≡N_{br} bond angle is roughly linear (174°), as is the average Re−C≡O bond angle (175°). However, the average Re−N≡C bond angle is only 166°. This smaller than expected bond angle is especially pronounced for the two Re moieties which are trans to each other with respect to the Fe center. These two Re fragments are bent away from the third Re center, presumably as a result of steric interactions. This steric hindrance between Re groups is probably the reason that the molecule crystallizes as the meridional isomer, as opposed to the facial one. It also raises the question of whether there is room for the addition of any further Re fragments to make the higher order $FeRe_n$ derivatives where n = 4, 5, or 6.

Selected bond length averages are also listed in Table 6. While the bridging M−CN−Mn (M = Cr, Mn, Fe, Co, Ni) is fairly common and has been structurally characterized by others, to our knowledge, the second- and third-row congeners M−CN−Tc and M−CN−Re remain relatively unexplored. The structure of $[Re(CO)_4(CN)]_3$ contains three Re−CN−Re units and appears to be the only crystal structure of M−CN−Re in the literature.[22] The average Re−NC and CN bond lengths in **4** are 2.16 and 1.13 Å, respectively, compared to 1.92 and 1.14 Å in $[Re(CO)_4(CN)]_3$. The only published crystal structure of an Fe−CN−M moiety in which M is a third-row metal seems to be the $[(NC)_5Fe(\mu\text{-}CN)Pt(NH_3)_4(\mu\text{-}CN)Fe(CN)_5]^{4-}$ anion reported by Bocarsly *et al.*[4] The average Fe−CN_{br} and Fe−CN_{non} bond lengths for **4** are 1.92 and 1.93 Å, respectively, compared with 1.88 and 1.92 Å for $[(NC)_5Fe(\mu\text{-}CN)Pt(NH_3)_4(\mu\text{-}CN)Fe(CN)_5]^{4-}$. The average bond distances listed above for **4** are in

(21) The equations used were: (a) R(F) = R1 = $\Sigma||F_o| - |F_c||/\Sigma|F_o|$; (b) wR($F^2$) = wR2 = $[\Sigma w(F_o^2 - F_c^2)^2/\Sigma w(F_o^2)^2]^{1/2}$; (c) S = goodness-of-fit on F^2 = $[\Sigma w(F_o^2 - F_c^2)^2/(n - p)]^{1/2}$, where n is the number of reflections and p is the number of parameters refined.

(22) Calderazzo, F.; Mazzi, U.; Pampaloni, G.; Poli, R.; Tisato, F.; Zanazzi, P. F. *Gazz. Chim. Ital.* **1989**, *119*, 241.

Table 5. Atomic Coordinates (x10^4) and Equivalent Isotropic Displacement Parameters (Å^2 × 10^3) for Compound **4**

atom label	*x*	*y*	*z*	U^a	atom label	*x*	*y*	*z*	U^a
Re(1)	6164 (1)	1226 (1)	2575 (1)	42 (1)	C(217)	−73 (27)	3863 (23)	4258 (19)	47 (9)
N(101)	6421 (18)	1049 (19)	1430 (14)	38 (6)	O(217)	−736 (20)	3981 (22)	4565 (14)	91 (10)
C(102)	6161 (28)	200 (29)	885 (22)	63 (11)	Re(3)	1492 (1)	4116 (1)	117 (1)	31 (1)
C(103)	6295 (25)	101 (22)	154 (22)	56 (10)	N(301)	2849 (18)	3961 (16)	−506 (12)	35 (6)
C(104)	6756 (23)	897 (23)	−66 (17)	40 (8)	C(302)	3608 (24)	4680 (21)	−595 (16)	42 (8)
C(105)	6998 (20)	1830 (21)	504 (18)	41 (8)	C(303)	4460 (21)	4576 (19)	−954 (14)	28 (7)
C(106)	9853 (23)	1888 (21)	1255 (16)	39 (7)	C(304)	4502 (24)	3629 (23)	−1267 (18)	51 (8)
C(107)	7122 (23)	2769 (22)	1851 (17)	42 (6)	C(305)	3699 (23)	2863 (21)	−1176 (16)	45 (7)
C(108)	7430 (22)	3694 (20)	1784 (16)	38 (7)	C(306)	2885 (21)	3019 (18)	−827 (15)	31 (6)
C(109)	7757 (23)	4504 (19)	2384 (17)	39 (7)	C(307)	1983 (25)	2293 (18)	−675 (17)	41 (8)
C(110)	7731 (22)	4393 (28)	3077 (17)	51 (10)	C(308)	1833 (25)	1268 (24)	−990 (17)	54 (10)
C(111)	7403 (23)	3459 (26)	3124 (19)	45 (9)	C(309)	1010 (28)	534 (20)	−925 (20)	54 (8)
N(112)	7055 (20)	2668 (20)	2529 (16)	51 (7)	C(310)	249 (28)	872 (22)	−535 (19)	62 (11)
C(113)	7014 (31)	932 (30)	−816 (18)	81 (31)	C(311)	402 (22)	1842 (19)	−244 (15)	35 (8)
C(114)	8115 (26)	5588 (19)	2345 (18)	53 (8)	N(312)	1216 (17)	2553 (14)	−304 (13)	32 (6)
C(115)	6051 (25)	1635 (23)	3618 (18)	44 (6)	C(313)	5428 (30)	3473 (28)	−1662 (21)	78 (12)
O(115)	5966 (24)	1749 (19)	4223 (14)	86 (9)	C(314)	863 (28)	−553 (19)	−1240 (20)	62 (9)
C(116)	5301 (32)	−89 (34)	2473 (20)	69 (12)	C(315)	347 (24)	4074 (21)	669 (17)	41 (8)
O(116)	4801 (22)	−908 (19)	2366 (17)	94 (11)	O(315)	−361 (19)	3981 (17)	1021 (15)	68 (7)
C(117)	7369 (33)	882 (32)	2846 (21)	76 (12)	C(316)	1916 (25)	5572 (23)	423 (15)	41 (8)
O(117)	8089 (26)	616 (25)	2971 (19)	112 (12)	O(316)	2122 (19)	6412 (15)	586 (14)	68 (8)
Re(2)	1002 (1)	3521 (1)	3615 (1)	39 (1)	C(317)	576 (23)	3966 (22)	−692 (16)	41 (7)
N(201)	2339 (19)	4439 (18)	4467 (13)	41 (6)	O(317)	−30 (18)	3793 (18)	−1241 (13)	72 (7)
C(202)	2740 (25)	4230 (25)	5031 (20)	53 (9)	Fe(1)	3698 (3)	2957 (3)	1717 (2)	26 (1)
C(203)	3643 (25)	4809 (26)	5513 (18)	48 (9)	C(1)	4429 (20)	2202 (18)	2093 (13)	20 (4)
C(204)	4147 (27)	5669 (25)	5385 (16)	52 (7)	N(1)	4913 (19)	1787 (16)	2283 (12)	35 (6)
C(205)	3783 (22)	5928 (20)	4844 (15)	40 (8)	C(2)	2805 (19)	3082 (18)	2503 (15)	22 (5)
C(206)	2887 (24)	5315 (21)	4378 (14)	37 (7)	N(2)	2224 (17)	3234 (17)	2933 (14)	37 (6)
C(207)	2411 (21)	5633 (20)	3785 (14)	30 (7)	C(3)	2965 (19)	3625 (16)	1262 (13)	17 (6)
C(208)	2923 (24)	6484 (21)	3643 (16)	42 (8)	N(3)	2518 (17)	3967 (16)	962 (12)	28 (4)
C(209)	2311 (31)	6624 (24)	3059 (18)	59 (10)	C(4)	4554 (22)	2835 (18)	902 (16)	28 (7)
C(210)	1404 (30)	5927 (31)	2673 (22)	88 (15)	N(4)	5016 (24)	2749 (21)	382 (15)	60 (8)
C(211)	1031 (27)	5094 (27)	2804 (19)	61 (10)	C(5)	4735 (22)	4167 (21)	2280 (17)	36 (7)
N(212)	1519 (20)	4918 (19)	3403 (14)	47 (7)	N(5)	5317 (24)	4917 (20)	2630 (16)	62 (9)
C(213)	5130 (25)	6301 (23)	5931 (15)	53 (7)	C(6)	2628 (22)	1720 (19)	1158 (15)	27 (6)
C(214)	2846 (36)	7615 (29)	2906 (31)	128 (23)	N(6)	1994 (21)	994 (19)	856 (14)	54 (8)
C(215)	−56 (21)	2878 (20)	2769 (15)	32 (7)	O(1S)	1751 (27)	−359 (30)	3556 (24)	127 (19)
O(215)	−723 (18)	2530 (15)	2241 (13)	61 (7)	C(1S)	2967 (40)	1076 (34)	3526 (35)	131 (28)
C(216)	722 (26)	2295 (30)	3895 (20)	57 (10)	C(2S)	1981 (28)	204 (28)	3197 (21)	96 (21)
O(216)	596 (24)	1640 (22)	4020 (20)	103 (11)	C(3S)	1202 (50)	−44 (49)	2514 (28)	153 (34)

[a] Equivalent isotropic *U* defined as one-third of the trace of the orthogonalized $\mathbf{U}_{ij}$ tensor.

Table 6. Representative Bond Distances (Å) and Bond Angles (deg) for Compound **4**

$Re(1)-N(1)_{CN\ bridge}$	2.17(2)	$Fe(1)-C(1)_{CN\ bridge}$	1.93(3)
$Re(1)-N(101)_{aromatic}$	2.16(2)	$Fe(1)-C(4)_{nonbr\ CN}$	1.94(3)
$Re(1)-C(117)_{trans\ CO}$	1.89(4)	$C(117)-O(117)_{trans\ to\ CN}$	1.17(4)
$Re(1)-C(116)_{cis\ CO}$	1.92(5)	$C(115)-O(115)_{cis\ to\ CN}$	1.12(3)
$C(1)-N(1)_{CN\ bridge}$	1.12(3)	$C(4)-N(4)_{nonbr\ CN}$	1.17(3)
C(1)−Fe(1)−C(3)	175(1)	C(1)−Fe(1)−C(2)	94(1)
Fe(1)−C(3)−N(3)	176(2)	C(2)−Fe(1)−C(3)	89(1)
Re(3)−N(3)−C(3)	160(2)	Re(3)−C(317)−O(317)	175(3)

Table 7. Observed and Calculated Intervalence Charge-Transfer Properties for Compounds **1**−**3** in Acetonitrile Solution[a]

property	**1**	**2**	**3**
$\bar{\nu}_{max}$ (cm^{-1})	20120	18420	17270
$\epsilon_{MM'CT}$ ($M^{-1}\ cm^{-1}$)	165	390	470
Δ (cm^{-1})	8740	7510	6150
H_{ab} (cm^{-1})	670	643	505
α (unitless)	0.033	0.034	0.029
$\Delta E°$ (V)[b]	1.32	1.05	0.76
$\Delta G°$ (kcal/mol)	30.4	24.2	17.5
χ (kcal/mol)	27.1	28.5	31.9
ΔG^* (kcal/mol)	30.6	24.4	19.1
$\Delta G'$ (kcal/mol)	0.11	0.16	1.6

[a] Abbreviations are defined in the text. Equations 1−5 were used to obtain values for the calculated parameters. [b] Calculated as the difference between E_{pa} for $Re^{II/I}$ and $E_{1/2}$ for $Fe^{III/II}$. This can only be considered as an estimate of the thermodynamic potential difference since neither of these redox waves were electrochemically reversible.

good agreement with these two earlier structures. The slightly shorter $Fe-CN_{br}$ distance in $[(NC)_5Fe(\mu\text{-}CN)Pt(NH_3)_4(\mu\text{-}NC)\text{-}Fe(CN)_5]^{4-}$ than in **4** can be attributed to the different oxidation state (+2) and the increased degree of Fe−CN back-bonding in the former complex. The average $Re-N_{arom}$ bond distance in **4** is 2.17 Å, in comparison with the 2.14 Å average of bpyRe-$(CO)_3L$, where L = BH_3CN^-, HCO_2^-, and $PF_2O_2^-$.[23] The observed Re−CO and CO bond averages for **4** are also in good agreement with similar complexes in the literature.[24]

Intervalence Charge-Transfer Properties. The energy of the MM′CT bands (E_{op}) for Compounds **1**−**3** decreases as the difference in redox potentials for the $Fe^{III/II}$ and $Re^{II/I}$ waves decreases, in agreement with simple Marcus−Hush theory given by eq 1, where χ is the reorganization energy. Assuming that the MV compounds behave as Robin and Day Class II compounds, the MV compounds can be modeled as shown in Figure 2 and eqs 2 and 3 can be used to predict the activation barriers to electron transfer in the thermodynamically unfavor-

(23) (a) Guilhem, J.; Pascard, C.; Lehn, J.-M.; Ziessel, R. *J. Chem. Soc., Dalton Trans.* **1989**, 1449. (b) Horn, E.; Snow, M. R. *Aust. J. Chem.* **1980**, *33*, 2369.

(24) Orpen, A. G.; Brammer, L.; Allen, F. H.; Kennard, O.; Watson, D. G.; Taylor, R. J. *J. Chem. Soc., Dalton Trans.* **1989**, S1.

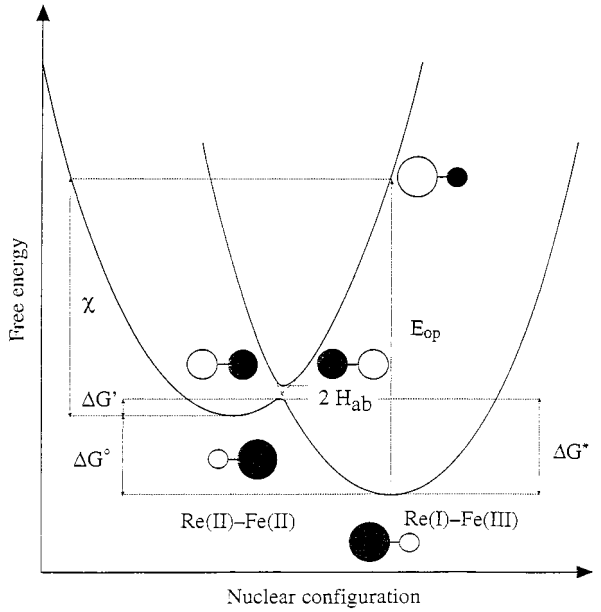

Figure 2. Potential energy diagram for the Re(I)-Fe(III) mixed-valence compounds. Abbreviations are defined in the text. The shaded and hollow circles represent the coordination spheres of the two metals, with the transferring electron occupying the shaded metal center. The metal with the higher oxidation state is shown by the smaller sized circle.

able (ΔG^*) and thermodynamically favorable ($\Delta G'$) directions, respectively, within the bridged complex. Furthermore, the magnitude of the electronic coupling (H_{ab}, cm^{-1}) can be estimated from the molar absorptivities of the MM′CT bands (ϵ, $M^{-1}\,cm^{-1}$), their energies ($\bar{\nu}$, cm^{-1}), their full-widths at half-maximum ($\Delta\bar{\nu}_{1/2}$, cm^{-1}), the degeneracy (g), and the distance the electron has to travel between them (estimated in this case as the crystallographic distance between the Fe and Re centers, 5.22 Å).[6i] The delocalization parameter (α) can be calculated from eq 5 and should be less than 0.25 for the MV compounds to be considered as Class II. The calculated parameters for Compounds **1**−**3** are shown in Table 7. The calculated delo-

$$\Delta G^* = \frac{E_{op}^2}{4\chi} \tag{2}$$

$$\Delta G' = \Delta G^* - \Delta G^\circ \tag{3}$$

$$H_{ab} = 0.0205\left(\frac{\epsilon\Delta\bar{\nu}_{1/2}}{\bar{\nu}g}\right)^{1/2}\left(\frac{\bar{\nu}}{r}\right) \tag{4}$$

$$\alpha = \sqrt{\frac{H_{ab}^2}{\bar{\nu}^2}} \tag{5}$$

calization parameters for the three MV species range from 0.029 to 0.034, well below the 0.25 upper limit for Class II MV compounds, indicating that the valences on the metal centers can be considered as essentially trapped. This is in good agreement with the values of α calculated for other multinuclear MV complexes which are bridged by cyanide linkages.[25] Additionally, the value of H_{ab} is less than 10% of that for the reorganization energy in each complex. Therefore, Marcus−Hush treatment of the intervalence charge transfer properties of these molecules is expected to yield reasonably accurate predictions of the electron transfer properties within these compounds. The relatively constant value for H_{ab} across the

(25) Pfennig, B. W. Ph.D. Dissertation, Princeton University, 1992.

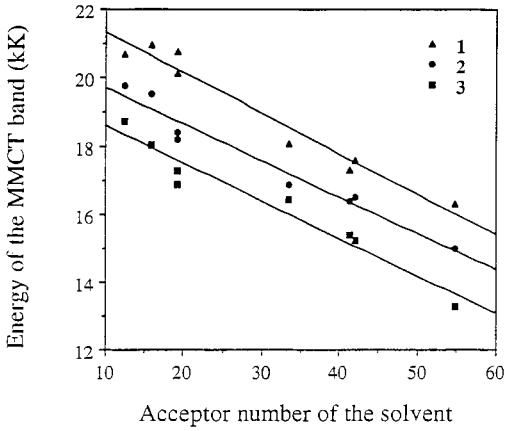

Figure 3. Solvent-dependence study of the energies of the MM′CT bands for Compounds **1**−**3** as a function of the Gutmann acceptor number of the solvent.

series of compounds is to be expected, given that the same metals are involved in the optical electron-transfer process and the internuclear separation is expected to be the same for each compound. The energies of the MM′CT bands for the series of compounds closely parallels the ground-state redox potential differences, yielding an average reorganization energy of 29.1 kcal/mol. By comparison, the reorganization energy for the symmetric MV compound $[(NC)_5Fe^{II}-CN-Fe^{III}(CN)_5]^{6-}$ in aqueous solution is 22.0 kcal/mol.[26] The calculated activation barriers for $Re^{I}\rightarrow Fe^{III}$ in the MV compounds vary from 19.1 to 30.6 kcal/mol and are all large enough that the transferring electron can be considered to be trapped on the Re center at room temperature; whereas the activation barriers for the reverse electron transfer from $Fe^{II}\rightarrow Re^{II}$ are all less than 2 kcal/mol.

The solvent-dependence of the intervalence charge-transfer bands for **1**−**3** was also investigated. These data are summarized in Table 3. The solvent can affect the barrier to electron transfer in one of two ways: (1) the reorganization energy is dependent on the solvent parameter according to eq 6, where D_{op} is the optical dielectric constant (equal to the square of the refractive index) and D_s is the static dielectric constant of the solvent; or (2) by changing the ground-state free energy difference, ΔG°, between the two redox isomers. Using the data in Table 3, it was observed that there was little or no correlation between E_{op} and $(1/D_{op} - 1/D_s)$ for the solvents investigated, but that there was a good relationship between E_{op} and the solvent's acceptor number (Figure 3). The acceptor number is based in

$$\chi = \chi_{in} + e^2\left(\frac{1}{2a_1} + \frac{1}{2a_2} - \frac{1}{r}\right)\left(\frac{1}{D_{op}} - \frac{1}{D_s}\right) \tag{6}$$

part on Gutmann's measurements of the redox potential of $(TBA)_3Fe(CN)_6$ in various solvents and reflects the ability of the solvent to accept electron density from the lone pair electrons on the cyanide nitrogens.[27] The larger the acceptor number, the more positive the $Fe^{III/II}$ redox couple is expected to be; whereas the oxidation potential of Re should remain relatively unaffected by the solvent. Therefore, as the acceptor number increases, ΔG° decreases, and E_{op} shifts to lower energies. The nearly linear relationship between E_{op} and acceptor number indicates that the predominant role of the solvent in determining the activation barrier in this series of MV compounds lies in the ΔG° term, rather than in the reorganization energy term.

(26) Glauser, R.; Hauser, U.; Herren, F.; Ludi, A.; Roder, P.; Schmidt, E.; Siegenthaler, H.; Wenk, F. *J. Am. Chem. Soc.* **1973**, *95*, 8457.
(27) Gutmann, V. *Electrochim. Acta* **1976**, *21*, 661.

Acknowledgment. The authors acknowledge Edward P. Vicenzi of the Princeton Materials Institute for determining the electron microprobe analysis. This work received financial support from the Camille and Henry Dreyfus Foundation in the form of a Faculty Start-Up Grant, the Committee on Grants at Franklin & Marshall College, the Hackman Scholars Program, and Vassar College.

Supporting Information Available: Tables S1−S6 listing all nonequivalent bond distances and bond angles, bond distances and bond angles involving H atoms, anisotropic displacement factors, and hydrogen atomic coordinates and isotropic displacement factors; and Figure S1, depicting the unit cell. This material is available free of charge via the Internet at http://pubs.acs.org.

IC9811751